Iron Loss Characteristics Evaluation Using a High-Frequency GaN Inverter Excitation

Wilmar Martinez, Shunya Odawara, and Keisuke Fujisaki

Toyota Technological Institute, Nagoya 4688511, Japan

Recently, novel magnetic materials have been developed for high-efficiency and high power density electric motors. In addition, next-generation semiconductor devices, like silicon carbide (SiC) or gallium nitride (GaN), have been introduced for power converters due to their high-frequency operation. Therefore, high-frequency operation of new magnetic materials is possible when they are driven by GaN or SiC inverters. Nevertheless, iron loss characterization of magnetic materials when they are excited by high-frequency signals have not been conducted yet. This paper introduces the iron losses characterization of a magnetic material at high carrier frequency excitation using a GANFET inverter. This characterization was carried out by the experimental evaluation of iron losses at carrier frequencies from 5 to 500 kHz at different deadtimes. As a result of the measurements, iron losses seem to have a trend to increase at high carrier frequencies and large deadtimes. In addition, filtering is introduced and it seems to be an effective technique for reducing iron losses.

Index Terms— **Gallium nitride, high frequency, inverter, iron losses, magnetic characteristic, sampling frequency.**

I. Introduction

POWER electronics circuits have been widely used in power conversion applications like electrical machines drives for their rapid response, controllability, and high efficiency [1]–[4]. Moreover, power converters have obtained remarkable improvements due to the introduction of next-generation semiconductors like silicon carbide (SiC) or gallium nitride (GaN). These new materials devices have outstanding characteristics of high-voltage and high-temperature operation, low ON-resistance, and fast switching [5]–[8]. With these semiconductors, high-frequency operation is possible achieving low switching losses, high power density, and cost reduction of magnetic components like reactors or transformers [1], [9], [10]. Nevertheless, for high-frequency operation, accurate loss calculation and measurements must be considered. Thus, in order to improve the total system efficiency, not only the semiconductors losses but also the magnetic material losses must be considered. Then, characterization of the magnetic components used in power converter circuits or in electric machines is important at a high-frequency operation.

Conventionally, in electrical machines, sinusoidal excitation has been used to evaluate magnetic characteristics of electromagnetic steel sheets. Then, with the introduction of power inverters, several studies of carrier frequency influence on magnetic materials have been conducted. Specifically, these studies approached the effect of carrier frequency and modulation index on the iron loss change. Nevertheless, most of these studies were conducted for low carrier frequency excitation (up to 20 kHz) [11]–[18] and one study that achieved 190 kHz [19]. Therefore, iron loss characterization on steel sheets is required for frequencies higher than 200 kHz when an inverter with next-generation devices is used.

It is known that iron losses decrease with the increased modulation index [14]. An increase in the switching frequency leads to a small reduction in the iron losses, but an increase in the switching losses in the inverter [19]. Moreover, it is known that high switching frequencies generate higher ringing noise (because of the resonance in the circuit) due to the parasitic components in the inverter that produce transient responses with large *dv/dt* in the switching devices. Consequently, ringing noise effect on iron-losses must be considered as well as filtering techniques to reduce these ringing noises.

The magnetic characterization and the source of iron loss in magnetic materials is important, because they can help power electronics and electric machines designers to improve their designs in order to achieve high efficiency in the total system (inverter, filter, and motor).

In this paper, iron loss characterization using a GaNFET inverter controlled by a 32 b DSP is presented. This characterization is conducted varying the carrier switching frequency from 5 to 500 kHz. Iron losses are evaluated with deadtimes of 100, 200, and 300 ns in the inverter circuit. For this evaluation, the device under test is a ring core made with steel sheets (35H300). Moreover, the effect of the ringing phenomenon on the iron losses is studied. Then, a low-pass (LP) filter is used for ringing reduction and its influence on the iron loss characteristics is evaluated as well.

II. Iron Loss Evaluation Method

A. Measurement System

Fig. 1 shows the measurement system used in this paper. This system is intended to excite a ring core made with electromagnetic steel sheets of the material 35H300 manufactured by Nippon Steel Company. This ring has two coils wound with round wire, the primary connected to the inverter, and the secondary for the voltage measurement. This secondary coil is used to avoid the voltage drop generated in the primary coil

Manuscript received March 10, 2017; revised May 2, 2017; accepted May 26, 2017. Date of publication June 7, 2017; date of current version October 24, 2017. Corresponding author: W. Martinez (e-mail: whmartinezm@unal.edu.co).

Color versions of one or more of the figures in this paper are available online at http://ieeexplore.ieee.org.

Digital Object Identifier 10.1109/TMAG.2017.2712683

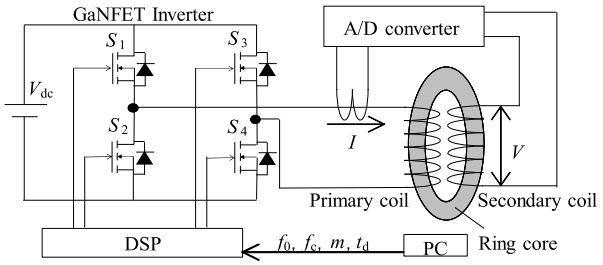

Fig. 1. Iron loss measurement circuit.

TABLE I
SPECIFICATIONS OF THE RING

Material	35H300
Outside Diameter d_o [mm]	127
Inside Diameter d_i [mm]	102
Height h [mm]	7
Number of turns of the primary coil N_1	254
Number of turns of the secondary coil N_2	254

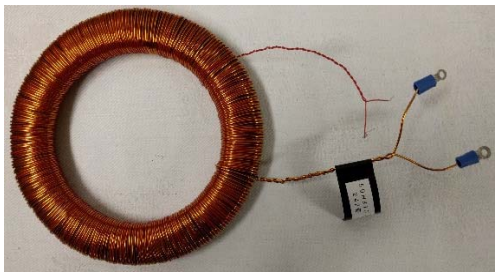

Fig. 2. Ring setup.

due to the primary current. When a secondary coil is used, the voltage can be measured without any current generation in the secondary, because there is no load connected to the secondary coil. Table I shows the ring specifications, and Fig. 2 shows the ring prototype.

This ring is excited by a full-bridge inverter constructed with four GaNFETs installed in two boards designed by Sanken Electric Corp. These switches are driven by a 32 b DSP manufactured by Texas Instruments. This DSP, with a 150 MHz of clock frequency, can achieve high-frequency signal generation suitable for the evaluation of magnetic materials. Table II shows the inverter parameters, and Fig. 3 shows the inverter prototype.

The measurement device used for these tests (A/D converter of Fig. 1) is a National Instruments' 14 b Oscilloscope/Digitizer capable of measuring with a maximum sampling frequency of 100 MS/s real time. With this scope, the primary-coil current is measured through a current probe (Hall effect—clamp type). This probe has a wide bandwidth from dc to 100 MHz and is capable to measure a maximum current of 30 A. In addition, the voltage of the secondary coil is measured using a differential voltage probe.

TABLE II
INVERTER PARAMETERS

Fundamental frequency f_o [Hz]	50
Carrier frequency f_c [kHz]	5-500
Modulation index m	0.5
Deadtime t_d [ns]	100-300
DC Voltage V_{dc} [V]	15-16
Maximum Flux Density in the ring [T]	1

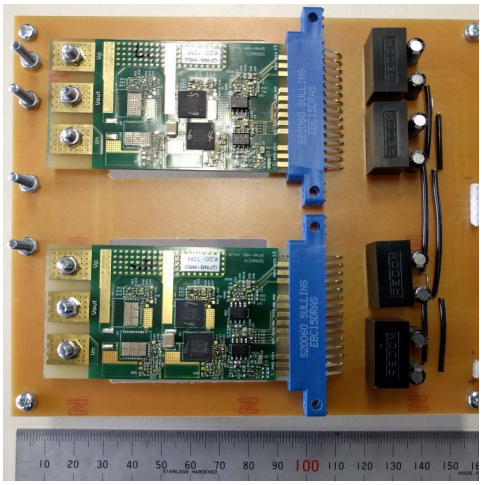

Fig. 3. Inverter setup.

Finally, in order to have a reference and a comparison of the iron loss evaluation of the selected material, a ring test under pure sinusoidal excitation of the ring is conducted. This sinusoidal tests are carried out using a function generator (TEXIO: FGX - 295) set with a frequency of 50 Hz. This signal is isolated and amplified with a linear amplifier (Takasago Works: BWS 120 - 2.5).

B. Experimental Method

The experimental tests are conducted with fixed modulation indices, as well as small variations of the dc Voltage. These parameters are determined to obtain a constant magnetic flux for all the measurements, and thereby have a fair comparison of the iron losses. In this case, the experimental tests were set to obtain 1 T of magnetic flux density. On the other hand, the carrier frequency and the deadtimes are varied from 5 to 500 kHz and from 100 to 300 ns, respectively.

In the case of the inverter, the dc voltage was set with a minimum voltage of 15 V, and the sinusoidal 50 Hz evaluation was conducted with a constant dc voltage of 5 V.

Then, the ring current and the secondary coil voltage are measured during one period of the fundamental frequency (20 ms). This data are saved using the digitizer and subsequently processed to obtain the iron loss value. Moreover, to have a more accurate measurement, this procedure is repeated five times for each carrier frequency and deadtime.

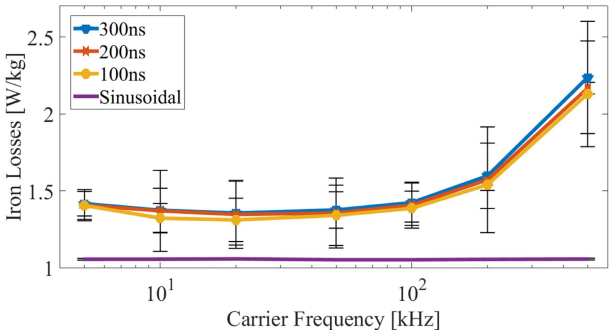

Fig. 4. Iron losses versus carrier frequency.

C. Iron Loss Calculation

In pursuance of evaluating the iron loss characteristics of a material, first, the magnetic flux density B and the magnetic field intensity H need to be described. In the evaluation system of Fig. 1, the current I flowing in the primary coil of the ring core and the induced voltage V generated on the secondary coil are measured. From the obtained I and V, H and B waveforms are obtained using (1) and (2) [11], respectively

$$H = \frac{N_1 I}{\text{MPL}} \tag{1}$$

$$B = \frac{1}{N_2 A} \int V dt. \tag{2}$$

MPL and A are the magnetic path length and the cross-sectional area of the ring core that can be calculated from the specifications of Table I. Then, the iron losses of the material W_{fe} can be calculated by integrating H and B as follows:

$$W_{\text{fe}} = \frac{f_o}{\rho} \int H \text{ dB} \tag{3}$$

where ρ is the density of the electromagnetic steel sheets (7650 kg/m^3).

III. Experimental Evaluation

Seven carrier frequencies (5, 10, 20, 50, 100, 200, and 500 kHz) and three deadtimes (100, 200, and 300 ns) are evaluated as well as the reference measurement of the sinusoidal case.

From (1)–(3) and the data obtained from each case, it was possible to calculate the iron loss density of each measurement. As it was mentioned before, several measurements of the same carrier frequency and deadtime were taken in order to see the deviation of the collected data. Fig. 4 shows the iron losses W_{fe} for each carrier frequency f_c obtained from the magnetic evaluation. Each dot in Fig. 4 represents the average of the five measurements that are collected. Also, the error bars (minimum and maximum points) of each measurement are shown. Moreover, the iron losses of the sinusoidal case are presented as well in Fig. 4 as a reference and point of comparison to the overall tests. It is important to have in mind that this value is independent of the carrier frequency, and it is only valid for 50 Hz.

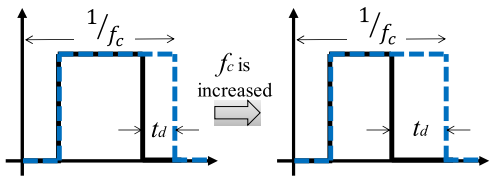

Fig. 5. Dead time effect on the voltage pulse.

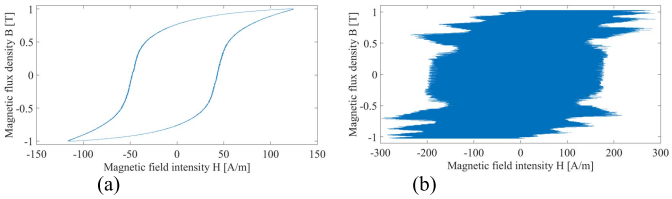

Fig. 6. $B - H$ curves comparison (sinusoidal and 500 kHz inverter).

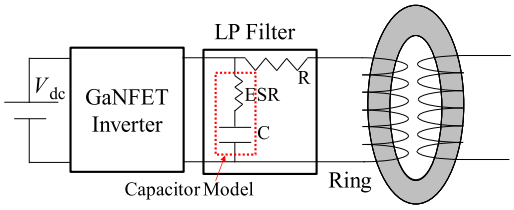

Fig. 7. Evaluation circuit with a filter.

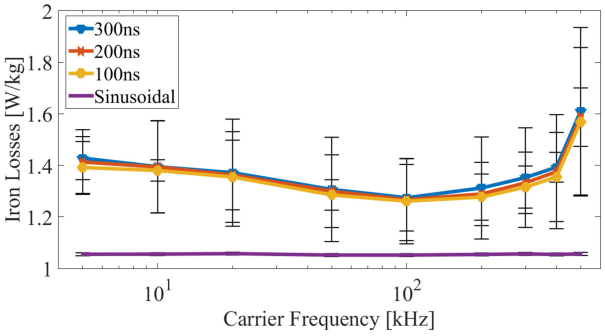

Fig. 8. Iron losses versus carrier frequency (with filtering).

As a matter of fact, the iron loss value obtained from the sinusoidal tests is close to the one presented by Nippon Steel Corporation in the datasheet of the selected material [20].

Fig. 4 appears to depict the increase of iron losses when the deadtime is increased. Specially, the higher the carrier frequency, the higher the difference between the iron losses at different deadtimes. This is generated by the portion of the deadtime in comparison to the total cycle, e.g., with a deadtime of 200 ns at a carrier frequency of 500 kHz and a duty cycle of 50%, the theoretical on-state will be 1 μs minus the deadtime during turn-ON and turn-OFF transients, and then the total ON-state will be reduced in a 40%. Consequently, a peak of current is generated, and therefore, the magnetic field intensity will be increased during the deadtime operation, and thereby the iron losses are increased.

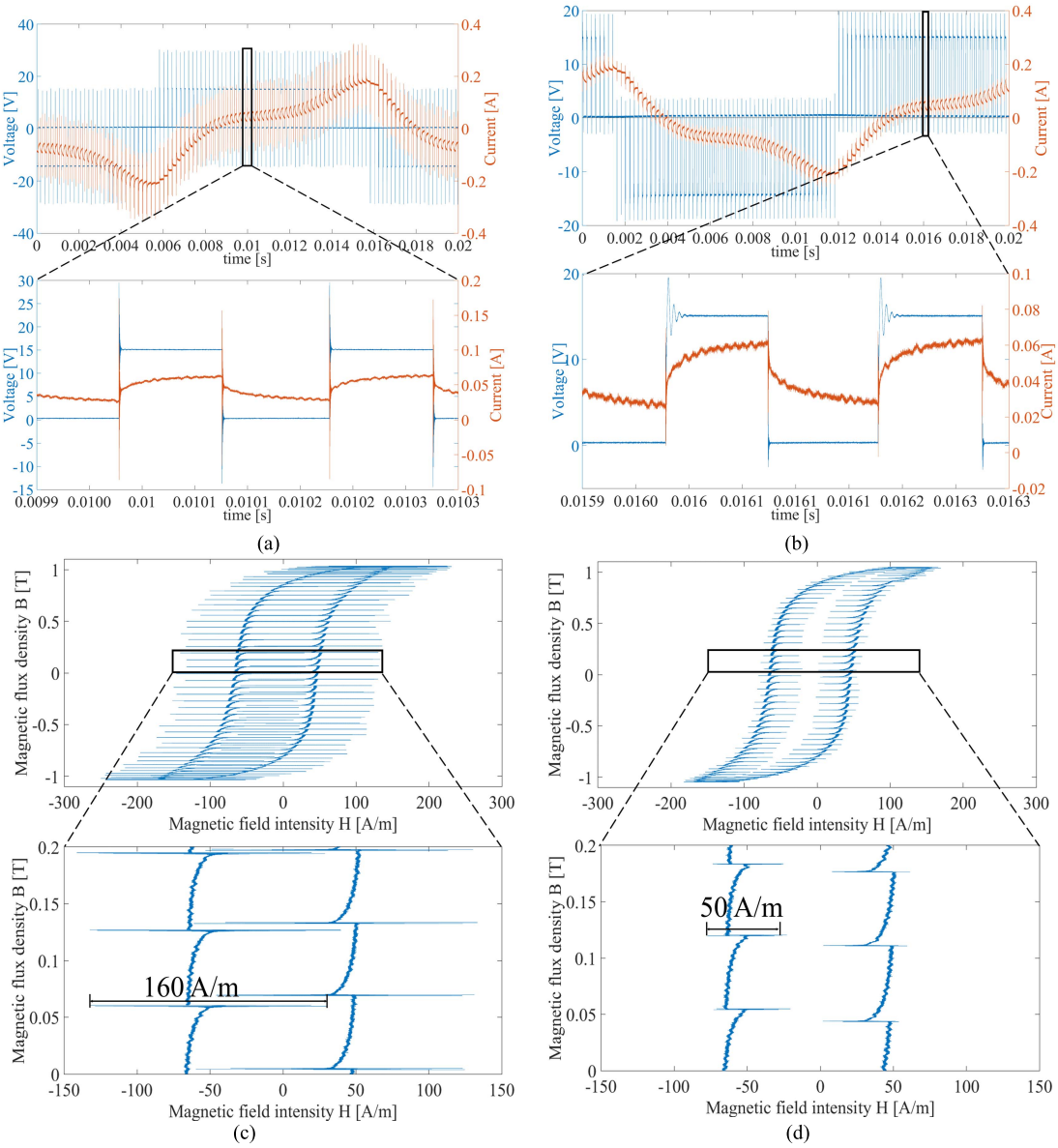

Fig. 9. Ring tests at 5 kHz 100 ns. (a) Waveforms without filter. (b) Waveforms with filter. (c) $B-H$ curve without filter. (d) $B-H$ curve with filter.

Similarly, Fig. 4 shows the carrier frequency effect on the iron losses, especially at high frequency. When the carrier frequency increases, a constant deadtime will occupy a bigger portion of the duty cycle, as shown in Fig. 5.

Then, the effective ON-time of the switching process is shorter due to the increase of the carrier frequency, and as it was explained before, the iron losses increase due to the change of the field intensity because of the change in the current.

Moreover, in the iron loss characterization, it is important to consider the effect of the parasitic components. As it is well known, the parasitic components presented in the semiconductors, PCB boards, wires, and so on make a bigger effect on the inverter operation when the switching frequency is increased. Thus, during the transient responses of the switching states, ringing noises with large surge voltages generate current spikes and therefore large changes of the field intensity ΔH. Fig. 6 shows the $B-H$ curves of the sinusoidal case and the inverter with a carrier frequency of 500 kHz. The difference between the field intensities of both the cases is evident.

IV. Filtering Evaluation

Considering the iron loss increase because of the ringing noise, a filtering evaluation was conducted to evaluate the iron loss reduction when ringing is reduced. Therefore, an LP filter was installed between the inverter and the ring, as shown in Fig. 7.

The intention of this LP filter is to attenuate the high-frequency components, and thereby to reduce the ringing during the transients of the switching operation in the GaNFETs. In this case, it was decided to use the internal resistance of the primary coil (R in Fig. 7) with a value of 0.56 Ω as well as a 220 nF ceramic capacitor. Consequently, the

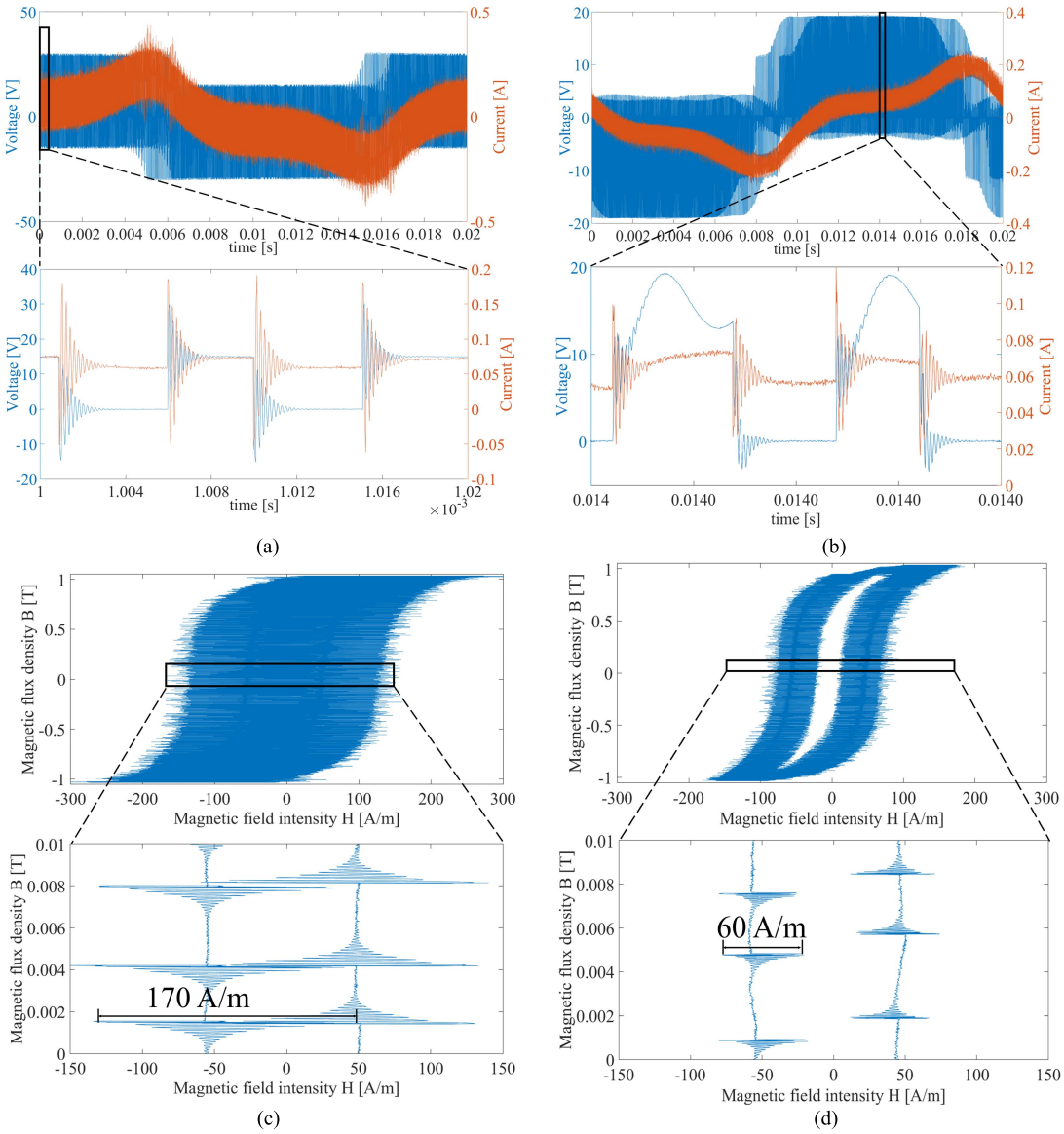

Fig. 10. Ring tests at 100 kHz 100 ns. (a) Waveforms without filter. (b) Waveforms with filter. (c) $B-H$ curve without filter. (d) $B-H$ curve with filter.

procedure explained in Section II was repeated, testing three deadtimes (100, 200, and 300 ns) and nine carrier frequencies (5, 10, 20, 50, 100, 200, 300, 400, and 500 kHz). Again, each case was measured five times for accuracy purposes. Thus, Fig. 8 shows the iron losses when the LP filter is installed in the circuit. Table III shows the reduction in each case of carrier frequency and deadtime.

Figs. 9–11 show the waveforms and $B-H$ curves of three cases (5, 100, and 500 kHz of carrier frequency) when the ring is excited by the inverter with and without filter. These figures depict the influence of the ringing reduction on the shape of the $B-H$ curve. In addition, the ΔH reduction is evident in each figure: 3.2 times at 5 kHz, 2.83 times at 100 kHz, and 2.3 times at 500 kHz. Moreover, it is possible to observe the increase of ΔH when the carrier frequency is increased (with and without filter), as it was mentioned in Section III.

TABLE III
IRON LOSS REDUCTION [%]

f_c [kHz]	5	10	20	50	100	500	500
t_d =100 ns	0.93	2.37	4.11	4.09	9.04	17.1	26.3
t_d =200 ns	0.86	1.21	1.53	4.39	9.95	17.8	26.8
t_d =300 ns	0.83	1.22	1.75	5.01	10.5	18.0	28.0

Conclusively, the effect of ringing in the iron losses and the effectiveness of the LP filter for reducing the ringing and the iron losses in the magnetic material are evident. The tests seem to show a reduction up to 28% at high carrier frequencies (see Table III).

Nevertheless, it is important to highlight that the loss reduction mentioned above is only produced in the ring core.

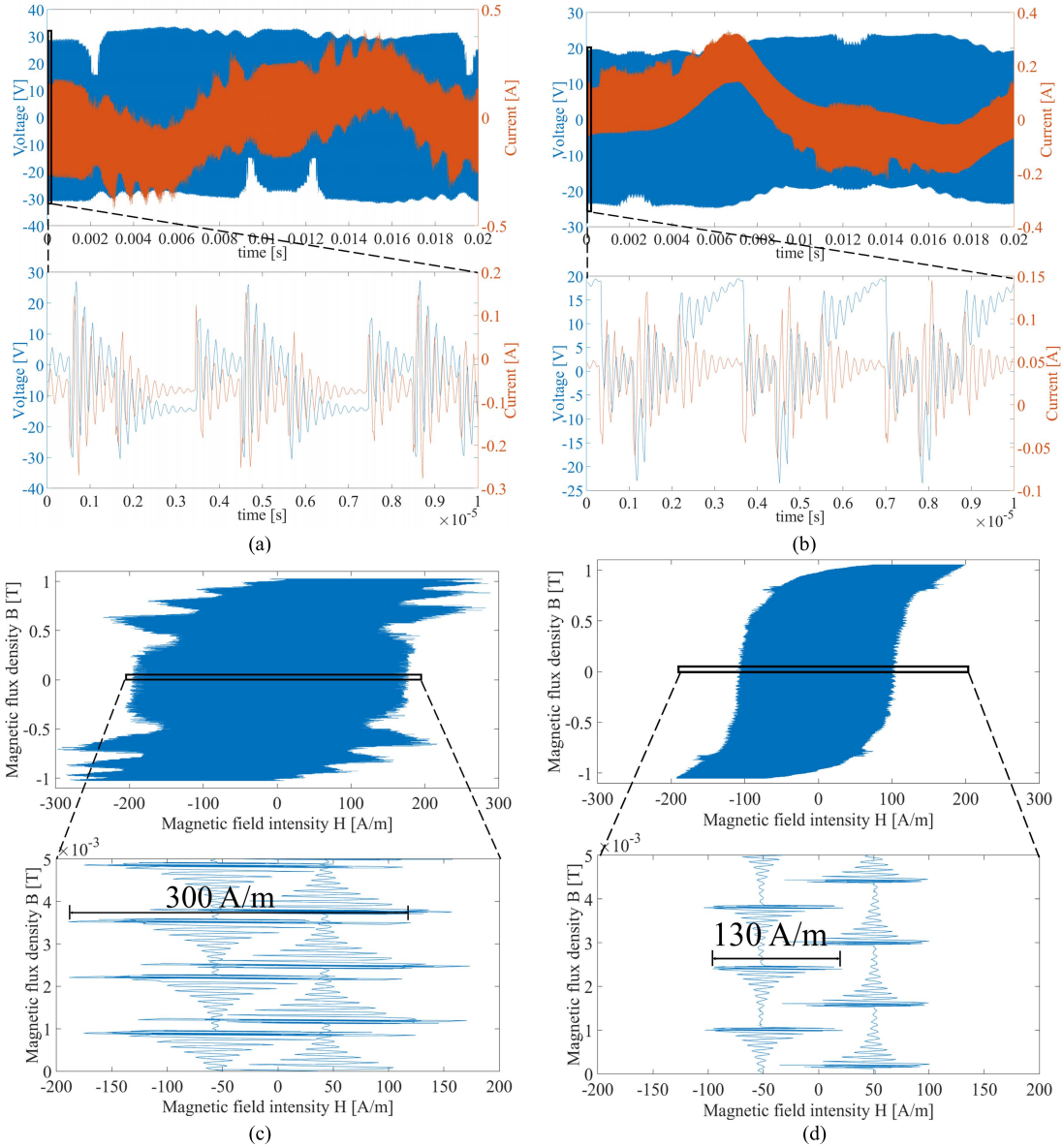

Fig. 11. Ring tests at 500 kHz 100 ns. (a) Waveforms without filter. (b) Waveforms with filter. (c) $B-H$ curve without filter. (d) $B-H$ curve with filter.

In fact, the installation of a LP filter introduces losses to the total system due to the parasitic components of the filter itself. As shown in Fig. 7, the filter's capacitor has its own parasitic components; especially, the equivalent series resistance (ESR) is a critical factor that affects the total efficiency. Fig. 12 shows the capacitance in parallel and the resistance in series of the 220 nF capacitor measured by an impedance analyzer.

Consequently, as the filter's capacitor is installed in parallel to the ring and the capacitor's ESR becomes quite smaller at high frequencies, the total impedance of the circuit's load becomes smaller, and therefore higher power is consumed from the source. Therefore, although the installation of an LP filter is effective for iron loss reduction, it compromises the total circuit efficiency.

V. Conclusion

In this paper, the influence of the carrier frequency and the deadtime on the iron loss characteristics of a ring core, made with steel sheets excited with a GaNFET inverter operated at high frequency switching, was studied and compared with the pure sinusoidal case.

As the deadtime and the carrier frequency f_o are increased, the effective ON-state voltage is reduced, and therefore current spikes are produced. This current change produces an increase in the change of the magnetic field intensity. Thus, iron losses are increased. In addition, due to these voltage and current spikes, and the ringing noise produced by the parasitic components presented in the circuit, iron losses are increased as well. Therefore, an LP filter was installed in the circuit for reducing the ringing voltage and attenuating the high-frequency components of the signals. Consequently, an iron loss reduction seems to be observable up to 28% at 500 kHz of carrier frequency and 300 ns of deadtime. Then, the circuit filtering is a good approach for reducing iron losses, especially at high carrier frequencies, but it might increase the total system losses. Thereby, an optimal design of the filter or the installation of a complex high-efficiency filter must be conducted to not compromise the total losses.

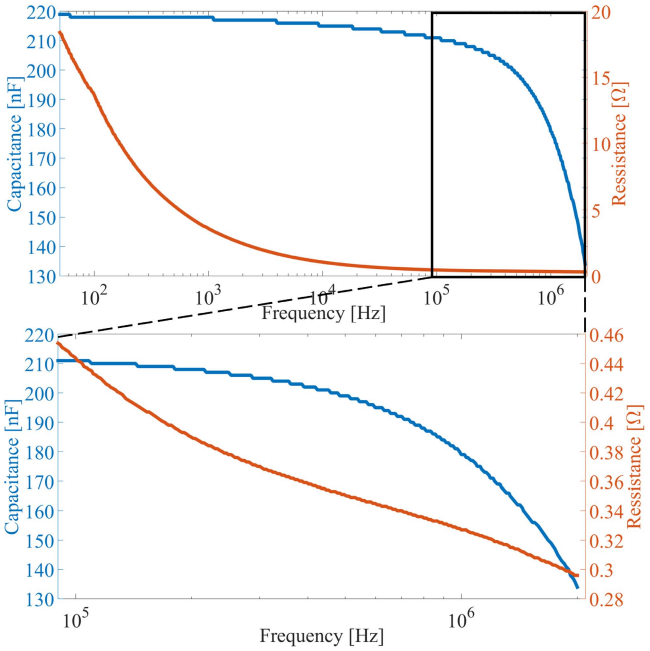

Fig. 12. Capacitor characteristics.

Finally, it is significant to mention the importance of the measurement equipment when a high-frequency procedure is conducted. Specifically, the A/D converter must have a high sampling frequency and the voltage and current detectors must have wide bandgap with good magnitude and phase characteristics.

ACKNOWLEDGMENT

This work was supported by Sanken Electric Corporation.

REFERENCES

[1] T. Morita *et al.*, "99.3% efficiency of three-phase inverter for motor drive using GaN-based gate injection transistors," in *Proc. 26th Annu. IEEE Appl. Power Electron. Conf. Expo. (APEC)*, Mar. 2011, pp. 481–484.

[2] W. Martinez, M. Yamamoto, J. Imaoka, F. Velandia, and C. A. Cortes, "Efficiency optimization of a two-phase interleaved boost DC-DC converter for electric vehicle applications," in *Proc. IEEE 8th Int. Power Electron. Motion Control Conf. (IPEMC-ECCE Asia)*, May 2016, pp. 2474–2480.

[3] M. Zeraoulia, M. E. H. Benbouzid, and D. Diallo, "Electric motor drive selection issues for HEV propulsion systems: A comparative study," in *Proc. IEEE Conf. Veh. Power Propuls.*, Sep. 2005, pp. 280–287.

[4] W. Martinez, C. A. Cortes, L. E. Munoz, and M. Yamamoto, "Design of a 200 kW electric powertrain for a high performance electric vehicle," *Ing. Invest.*, vol. 36, no. 3, pp. 66–73, 2016.

[5] F. Xu, B. Guo, L. M. Tolbert, F. Wang, and B. J. Blalock, "Evaluation of SiC MOSFETs for a high efficiency three-phase buck rectifier," in *Proc. 27th Annu. IEEE Appl. Power Electron. Conf. Expo.*, Feb. 2012, pp. 1762–1769.

[6] M. Yamamoto, "Full SiC soft switching inverter—Stability performance for false turn on phenomenon," in *Proc. 10th Int. Conf. Power Electron. Drive Syst. (PEDS)*, Apr. 2013, pp. 159–164.

[7] K. Shah and K. Shenai, "Performance evaluation of point-of-load chip-scale DC-DC power converters using silicon power MOSFETs and GaN power HEMTs," in *Proc. IEEE Green Technol. Conf. (IEEE-Green)* Apr. 2011, pp. 1–5.

[8] F. Hattori, H. Umegami, T. Yoshida, and M. Yamamoto, "Drive loss analysis and comparison of capacitor-less gate drive circuit for GaN FETs with capacitor type gate drive circuits," in *Proc. 10th Int. Conf. Power Electron. Drive Syst. (PEDS)*, Apr. 2013, pp. 1301–1305.

[9] J. Everts, J. Das, J. Van den Keybus, J. Genoe, M. Germain, and J. Driesen, "A high-efficiency, high-frequency boost converter using enhancement mode GaN DHFETs on silicon," in *Proc. IEEE Energy Convers. Congr. Expo.*, Sep. 2010, pp. 3296–3302.

[10] H. Umegami, F. Hattori, Y. Nozaki, M. Yamamoto, and O. Machida, "A novel high-efficiency gate drive circuit for normally off-type GaN FET," *IEEE Trans. Ind. Appl.*, vol. 50, no. 1, pp. 593–599, Jan./Feb. 2014.

[11] S. Odawara, D. Kayamori, and K. Fujisaki, "Influence of sampling frequency on magnetic characteristic evaluation under inverter excitation," *IEEJ Trans. Fundam. Mater.*, vol. 135, no. 7, pp. 385–390, 2015.

[12] K. Terashima, K. Wada, T. Shimizu, T. Nakazawa, K. Ishii, and Y. Hayashi, "Evaluation of the iron loss of an inductor based on dynamic minor characteristics," in *Proc. Eur. Conf. Power Electron. Appl.*, Sep. 2007, pp. 1–8.

[13] K. Yamazaki and Y. Kanou, "Rotor loss analysis of interior permanent magnet motors using combination of 2-D and 3-D finite element method," *IEEE Trans. Magn.*, vol. 45, no. 3, pp. 1772–1775, Mar. 2009.

[14] A. Boglietti, P. Ferraris, M. Lazzari, and F. Profumo, "Effects of different modulation index on the iron losses in soft magnetic materials supplied by PWM inverter," *IEEE Trans. Magn.*, vol. 29, no. 6, pp. 3234–3236, Nov. 1993.

[15] A. Boglietti, P. Ferraris, M. Lazzari, and F. Profumo, "Iron losses in magnetic materials with six-step and PWM inverter supply (induction motors)," *IEEE Trans. Magn.*, vol. 27, no. 6, pp. 5334–5336, Nov. 1991.

[16] Z. Gmyrek, A. Boglietti, and A. Cavagnino, "Estimation of iron losses in induction motors: Calculation method, results, and analysis," *IEEE Trans. Ind. Electron.*, vol. 57, no. 1, pp. 161–171, Jan. 2010.

[17] A. Boglietti, P. Ferraris, M. Lazzari, and M. Pastorelli, "Change of the iron losses with the switching supply frequency in soft magnetic materials supplied by PWM inverter," *IEEE Trans. Magn.*, vol. 31, no. 6, pp. 4250–4252, Nov. 1995.

[18] H. Kaihara *et al.*, "Effect of carrier frequency and circuit resistance on iron loss of electrical steel sheet under single-phase full-bridge PWM inverter excitation," *IEEE Trans. Magn.*, vol. 48, no. 11, pp. 3454–3457, Nov. 2012.

[19] T. Tanaka, S. Koga, R. Kogi, S. Odawara, and K. Fujisaki, "High-carrier-frequency iron-loss characteristics excited by GaN FET single-phase PWM inverter," *IEEJ Trans. Ind. Appl.*, vol. 136, no. 2, pp. 110–117, 2016.

[20] *Non-Oriented Electrical Steel Sheets*, Nippon Steel & Sumitomo Metal Corporation, Tokyo, Japan, 2015.